Performance of a submerged adsorption column compared with conventional fixed-bed adsorption

Md. Maksudur Rahman Khan[a,b,*], Md. Wasikur Rahman[a],
Md. Salatul Islam Mozumder[b], Kaniz Ferdous[b], Huei Ruey Ong[a], Kar Min Chan[a],
D.M. Reddy Prasad[c]

[a]*Faculty of Chemical and Natural Resources Engineering, Universiti Malaysia Pahang, Kuantan 26300, Pahang, Malaysia,
Tel. +6095492872; Fax: +6095492889; email: mrkhancep@yahoo.com (M.M.R. Khan), Tel. +60109396513;
email: wasikurjstu@gmail.com (M.W. Rahman), Tel. +60177742637; email: roi_rui86@hotmail.com (H.R. Ong),
Tel. +60129830910; email: karminchan@live.com.my (K.M. Chan)*
[b]*Department of Chemical Engineering and Polymer Science, Shahjalal University of Science and Technology, Sylhet 3114,
Bangladesh, Tel. +880 1732291688; email: salatulislam@yahoo.co.in (M.S.I. Mozumder), Tel. +880 1711103660;
email: engr_kaniz@yahoo.com (K. Ferdous)*
[c]*Department of Engineering, College of Applied Sciences, Post box–135, Sohar 311, Oman,
Tel. +96824885512; email: dmrprasad@gmail.com*

ABSTRACT

Submerged adsorption (SA) process has been explored in this context for the first time as a dynamic and effective approach, comparable to the conventional fixed-bed adsorption. Various design parameters like breakthrough time (t_b), adsorption capacity (q_{eq}), and effective bed height (H_B) of the adsorption columns were determined for different flow patterns, e.g. up-flow and down-flow. A fixed bed of jackfruit (*Artocarpus heterophylus*) leaf powder, already proved by our group as an efficient, cost-effective adsorbent for the removal of methylene blue from water in continuous mode using fixed-bed column, was selected for this study. The design basis of the adsorption columns were regarded as different bed depths (H_T = 5–10 cm), flow rates (Q = 20–60 mL/min), and initial dye concentrations (C_0 = 300–500 mg/L), for the experiment. With decreasing flow rates as well as increasing bed height and initial dye concentration for any flow arrangement, adsorption capacity of the column increased as the breakthrough time and usable bed height increased. Moreover, adsorption columns with up-flow showed better performance than down-flow pattern may be due to increasing q_{eq} and H_B up to 40 and 20%, respectively. Comparing design parameters of SA column to conventional FBA found that q_{eq} increased up to 22% as well as H_B and t_b increased corresponding to 9–14% and 20–86%, respectively. The experimental data were fitted with Thomas model and correlated with theoretical breakthrough curves, which pointed out the evidence of the effective design approach.

Keywords: Submerged adsorption module; Methylene blue; Low-cost adsorbent; Breakthrough analysis; Adsorption column design; Thomas model

*Corresponding author.

1. Introduction

Submerged adsorption (SA) concept arises from the submerged membrane adsorption (SMA) that is a valuable tool for liquid–solid separation. Membrane separation process has emerged as an innovative wastewater treatment technology. However, its application at present is limited due to its high cost of installation and its long-term operational difficulty. Membrane fouling is a major obstacle to the successful operation of the membrane separation process. The membrane processes such as reverse osmosis and nanofiltration can remove most of the pollutants, including dissolved organics [1], but their operational costs are high because of the high energy requirements and membrane fouling. Micro or ultrafiltration is a cost-effective option, but they are unable to remove dissolved organic materials due to their larger pore sizes [2].

Further advancement in membrane technology, especially known as SMA bioreactor, is expected to remove a superior amount of organic pollutants [3]. This is due to the fact that traces of adsorbent added in a membrane bio-reactor increase the organic pollutant removal capacity. The SMA bioreactor system can reduce biofouling of reverse osmosis membrane by eliminating biodegradable organic materials. It is robust and convenient due to reduced usage of chemicals (coagulants and biocides), and requires low energy consumption [4]. However, the process suffers from drawback of complexity of the process, environmental pollution, intermittent flow, readily blocked, frequent maintenance, etc.

Based on the above idea and considering the technological limitations, we propose a new, dynamic, cost-effective and eco-friendly process defined as submerged adsorption process. The process is also comparable to the conventional fixed-bed adsorption (FBA) technique. A number of process parameters need to be studied for successful adsorption process such as column design, properties of adsorbents and adsorbates, methods applied, continuous or batch flow, etc. [5–8].

In the last decade, various low-cost adsorbents have been explored to remove dye stuffs from industrial wastewater such as cedar sawdust [9], rice husk [10], hazelnut shell [11], peanut hull [12], lemon peel [13], perlite [14], kaolinite [15], neem leaf powder [16], fly ash [17], and clay [18]. Most of the authors evaluated the equilibrium and kinetic parameters based on batch experiments. However, equilibrium data are not useful when the process is operated in a fixed-bed system due to dynamic nature and inherent complexity of the system. Therefore, equilibrium studies of a process are needed to be performed in order to find out the design parameters of the system using adsorption columns.

Fluidization is very important from an industrial point of view. Liquid–solid fluidization process is widely utilized in water treatment and the operation involved may include adsorption. In the FBA, usually the influent is fed to the top [19] or bottom [17] of the column using a pump to maintain a fixed flow rate. The comparison between these two types of flow systems has not yet been reported in the literature. Usually, it is assumed that both the patterns should give the same results. Nevertheless, higher pressure drop at the bottom [20], voidage in the adsorbent particles [21], and expansion properties of the bed [22] impose us to think different. The breakthrough time and the dynamic equilibrium capacity are important parameters for designing the FBA columns that are affected by the surface utilization of the adsorbent in the fixed bed. Hence, the flow patterns should have an impact on the surface utilization of the fixed-bed column [23,24]. In the present study, jackfruit leaf powder (JLP) has been used as an adsorbent for the removal of methylene blue (MB) from its aqueous solution [5]. MB is selected as a model compound in order to evaluate the capacity of JLP for the removal of dye (MB) from aqueous medium. SA and conventional FBA experiments have been conducted with JLP–MB system using up-flow arrangement (UpF) and down-flow arrangement (DoF). Effects of column height (H_T), flow rate (Q), and initial dye concentration (C_0) have been investigated. The column data have been fitted with Thomas model, and the model parameters have been extracted. Additionally, the breakthrough time and the equilibrium capacities of the adsorption beds (5 and 10 cm) of SA have been compared with that of the conventional FBA process regarding different flow arrangements.

2. Materials and methods

2.1. Preparation of adsorbent

JLP was employed as an adsorbent for the removal of MB from aqueous solution. Jackfruit leaves were collected from Sylhet, Bangladesh, and thoroughly washed to remove dirty impurities. The washed leaves were successively dried in an oven at 105°C for about 16 h, crushed into fine particles, and the powder was boiled to completely remove lignin and coloring components present in the leaves. Finally, the powder was dried at 105°C for about 20 h and used for the whole experiment. The chemical and physical properties of the JLP were studied (Table 1) following the

Table 1
Physicochemical properties of JLP used in the experiment

Properties	Experimental value
Moisture content (%)	10.11
Ash content (%)	2.67
BET surface area (m^2/g)	507
Pore volume (cm^3/g)	0.78
Particle size (μm)	150–250

method reported elsewhere [25]. Specific surface area based on N$_2$ physisorption was measured using Brunauer–Emmett–Teller (BET) (Model: ASAP 2010, Micromeritics) method. The samples were degassed at 100°C for 2 h prior to the sorption measurement.

2.2. Preparation of adsorbate

MB, a cationic dye, used in this study was purchased from Merck (Germany) and employed as received. The stock solution of MB was prepared by dissolving exact amount of dye in distilled water to the concentration of 1 g/L. All experimental solutions were prepared by diluting the stock solution with distilled water in accurate proportions needed for initial dye concentrations.

2.3. Experimental setup

2.3.1. Submerged adsorption column

The schematic diagram of the SA column with UpF and DoF is shown in Fig. 1. A polyvinyl chloride (PVC) column with 4 cm internal diameter and 20 cm height was used to run the SA system. The column was packed with JLP adsorbent between two supporting layers of pre-equilibrated glass wool. For each run, 10 g of the adsorbent was used and the bed height was taken as 5 cm.

The column was submerged into a wastewater-containing tank at different depths. The static head was used to flow the influent through the column. Both UpF and DoFs are possible for this system. For UpF, the outlet pipe was fixed at the top of the column and for DoF, it was at the bottom of the column. In the present work, a single column was used to evaluate the performance of the unit, but it is possible to use a number of columns in series/parallel connection by submerging them into a tank. The column was submerged at a depth of 100 cm and a flow rate of 20 mL/min was achieved. The change in flow rates (20–40 mL/min) was achieved by changing the submerged depth of the column. The wastewater was
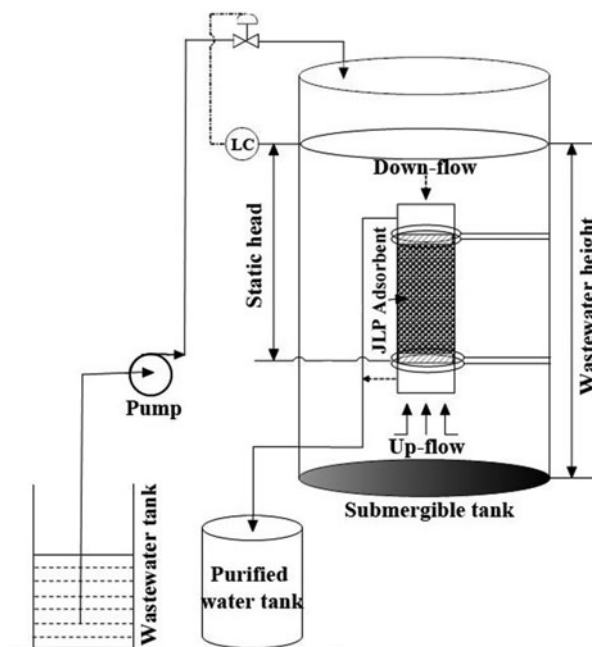

Fig. 1. Schematic diagram of the submerged adsorption system with up-flow (solid lines) and down-flow (dashed lines) arrangements.

continuously fed to the container to keep the static head constant. The initial dye concentrations were applied in the range of 300–500 mg/L. The whole process was controlled by a level controller (LC) connected with a control valve that controls the inlet flow to the column. The sensor collects signals from the process that are transmitted to the transmitter in order to convert them into standard one and send to the controller for the final action. While the operation was going on, the samples were collected at certain time intervals and the concentration of the dye was determined using UV–visible spectrophotometer (UV–1601, Shimadzu, Japan) at the wavelength of 664.5 nm at which the maximum absorbance was observed. The temperature and pH of all the experiments were maintained at 28 ± 2°C and 6.8 ± 0.2, respectively.

2.3.2. FBA column

FBA experiments were conducted in a PVC tube of internal diameter of 4 and 50 cm in length for UpF and DoF. The experimental setup is almost the same as shown in Fig. 1 for SA system excluding the tank arrangement. Moreover, the column beds were made by 10 and 20 g of JLP loaded for bed heights of 5 and 10 cm, respectively. An adjustable plunger was attached at the top of the column to maintain uniform static head. MB-containing wastewater was charged

through the column in the UpF and DoF with different flow rates with a pump (DENG YUAN–Diaphragm pump, Type–2500). The identical experimental conditions were followed as employed for SA system, e.g. flow rates, initial dye concentrations, sample characterization, etc. The operation was continued until the effluent MB concentration exceeded ~99.5% of its initial concentration.

2.4. Mathematical modeling for fixed-bed column studies

The column performances were studied by breakthrough curves of the continuous fixed-bed system. Breakthrough curves, in general, are expressed in terms of inlet dye concentration (C_0), outlet dye concentration (C), or normalized concentration which is defined as the ratio of effluent to influent dye concentration (C/C_0) as a function of volume or time of effluent for a given bed height. Effluent volume (V_{eff}) can be calculated as [6,26]:

$$V_{eff} = Qt \,(\text{mL}) \tag{1}$$

where t and Q are the total flow time (min) and volumetric flow rate (mL/min), respectively. Contact time is a vital parameter in the design of sorption columns and is often expressed in terms of the empty bed contact time (EBCT). EBCT affects the shape of the breakthrough curve and the volume to breakthrough. This is determined by Eq. (2):

$$\text{EBCT} = \frac{V_C}{Q} = \frac{AH_T}{Q} \,(\text{min}) \tag{2}$$

where V_C is the volume of sorbent on the bed, A is the cross-sectional area of the column, and H_T is the total bed height.

The performance of a fixed bed can be further evaluated in terms of the adsorbent usage rate, U_r, defined as the weight of adsorbent saturated per unit volume of adsorbate solution treated. U_r is given by:

$$U_r = \frac{m_c}{V_b} \,(\text{g/L}) \tag{3}$$

m_c and V_b, in the equation, correspond to the mass of adsorbent in the column and the volume of solution treated at breakthrough.

The total adsorbed capacity (q, mg/g) of MB cation in the column for a given feed concentration and flow rate is calculated as

$$q = \frac{C_0 Q A}{1,000w} = \frac{C_0 Q}{1,000w} \int_0^{t_t} \left(1 - \frac{C}{C_0}\right) dt \,(\text{mg/g}) \tag{4}$$

where w is the amount of adsorbent in the bed and t_t is the total time that is required to reach equilibrium with total bed.

Bed exhaustion time (t_e), the time at which the concentration of the dye in the effluent reached ~99.5% of the initial dye concentration, is calculated as:

$$t_e = \int_0^{t_t} \left(1 - \frac{C}{C_0}\right) dt \,(\text{min}) \tag{5}$$

The time equivalent usable capacity of the bed is generally determined up to breakpoint time. The breakthrough point can be taken as the point, at which the effluent concentration reaches a particular concentration, i.e. C/C_0 might be 5% [5], also considered in this work. The time equivalent to the usable capacity (t_u) is also defined as the time at which the effluent concentration reaches its maximum permissible level and can be calculated as

$$t_u = \int_0^{t_b} \left(1 - \frac{C}{C_0}\right) dt \,(\text{min}) \tag{6}$$

The value of t_u is usually very close to that of t_b, the time at which the concentration of the dye in the effluent reached at 3–5% of the influent concentration [27,28]. The ratio t_u/t_t is the function of the total bed capacity or the length utilized up to breakpoint. Hence, for a total bed length of H_T, the length of bed used up to the breakpoint (H_B) can be determined by

$$H_B = \frac{t_u}{t_t} H_T \,(\text{cm}) \tag{7}$$

The length of the mass transfer zone (H_{UNB}), also called as critical bed length, can be calculated from the breakthrough curves as follows:

$$H_{UNB} = \left(1 - \frac{t_u}{t_t}\right) H_T \,(\text{cm}) \tag{8}$$

A number of mathematical models have been developed that predict the mass- transfer zone as well as concentration–time profiles or breakthrough curves

in the bed. The Thomas or reaction model, which assumes Langmuir isotherm of adsorption–desorption, and no axial dispersion is derived with the adsorption that the rate driving force obeys second-order reversible reaction kinetics [29]. The model can be represented as follows:

$$\frac{C}{C_0} = \frac{1}{1 + \exp\left(\frac{k_{TH}}{Q}(q_{eq}X - C_0V_{eff})\right)} \tag{9}$$

where k_{TH} is the Thomas rate constant (mL/min mg), q_{eq}—maximum solid–phase concentration of the solute (mg/g), and X—the mass of adsorbent (g). A plot of C/C_0 vs. time, t (V_{eff}/Q) was employed to determine the values of k_{TH} and q_{eq} by fitting the experimental data followed by Eq. (9). The deviation (%) between the experimental and theoretical times for breakthrough can also be calculated as

$$\varepsilon = 100\left(\frac{t_{b,\,exp} - t_{b,\,cal}}{t_{b,\,exp}}\right) \tag{10}$$

3. Results and discussion

3.1. Performance of FBA module

3.1.1. Effect of bed height

The column experiments were conducted with 300 mg/L dye solutions at bed heights (H_T) of 5 and 10 cm with constant flow rate of 30 mL/min. The S-shaped breakthrough curves as obtained were shown in Fig. 2. The design and operating parameters are summarized in Table 2.

The breakthrough time increased from 210 to 780 min with an increase of bed height from 5 to 10 cm. Similar results have been reported by other researchers [30,31]. Lim and Aris [6] reported that longer bed delayed the breakthrough time (t_b) of the adsorbent, which means the bed is able to operate for a longer period without changing the adsorbent. For the shorter bed, in contrast, the t_b approached faster; hence, the performance declined [32]. The experimental breakthrough data were fitted with Eq. (9) to evaluate the Thomas rate constant (k_{TH}) and the theoretical breakthrough curve is shown as dense line in Fig. 2. It showed relatively good agreement between the experimental breakthrough curves and the theoretical values based on Thomas model. Fig. 2 indicates that the Thomas model can be used as a suitable mathematical representation of the MB–JLP adsorption system in a column. The maximum bed capacities for
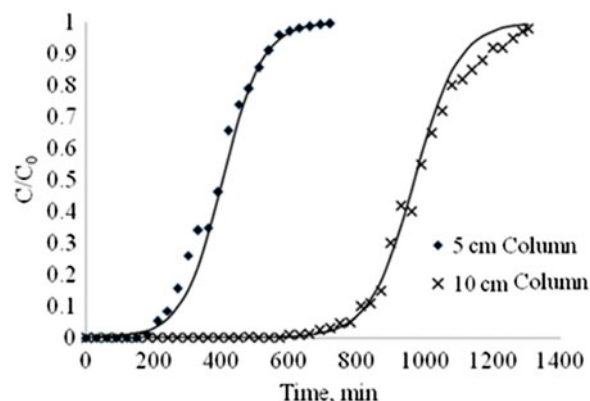

Fig. 2. Effect of bed heights of FBA: breakthrough curves of MB removal by JLP adsorbent predicted by Thomas model for up-flow mode with different bed heights (H_T = 5 and 10 cm) at C_0 = 300 mg/L and Q = 30 mL/min (symbols and lines correspond to experimental and theoretical values based on Eq. (9)).

different bed heights, 5 and 10 cm, were found to be 181 and 203 mg/g, respectively. The fact behind the increase in adsorption bed capacity (q_{eq}) with bed height (H_T) is due to the increase in adsorbent doses in larger bed which provides greater surface area (or adsorption sites). Moreover, a delayed breakthrough time of the pollutant leads to an increase in the volume of solution treated [5,8]. However, increasing the bed height does not affect k_{TH} (0.05 mL/mg min) for MB–JLP system in the column. The usable bed height (H_B) became approximately two times higher with the increase in total bed height (H_T), but the mass transfer zone (H_{UNB}) remained unchanged. The similar concept is recognized as an important design parameter and employed to scale up the adsorption column from the laboratory to pilot level [33].

3.1.2. Effect of volumetric flow rates

A column with UpF and DoF arrangements was studied at C_0 = 500 mg/L, H_T = 5 cm, diameter of 4 cm, and various volumetric flow rates (Q). The experimental and theoretical breakthrough curves were predicted using Thomas model, presented in Fig. 3(a) and (b). The flow rates were varied from 20 to 60 mL/min for UpF and 20 and 30 mL/min for DoF. The results are summarized in Table 2. It shows that a decrease in volumetric flow rate at a constant height increases the breakthrough time (t_b) and hence the volume of solution treated at the breakthrough point due to an increase in the EBCT. The breakthrough time for Q = 20, 30, 40, and 60 mL/min and C_0 = 500 mg/L was found to be 205, 115, 78, and 50 min, respectively for

Table 2
Adsorption column design parameters evaluated by Thomas model based on breakthrough curves of FBA and submerged adsorption of MB–JLP system for various operating conditions

| Operating parameters			Design parameters		Thomas model				EBCT (min)	U_r (g/L)
Conditions	Q (mL/min)	C_0 (mg/L)	t_b (min)	H_B (cm)	k_{TH} (mL/mg min)	q_{eq} (cal.) (mg/g)	q (exp.) (mg/g)	ε		
Fixed-bed adsorption column										
UpF, 5 cm	30	300	210	2.5	0.052	181	189	−9.5	2.09	3.17
UpF, 10 cm			780	7.48	0.051	203	234	0.6	4.18	1.71
UpF, 5 cm	20	500	205	2.1	0.022	273	269	9.7	3.14	4.89
	30		115	1.6	0.026	269	267	−13.05	2.09	5.8
	40		78	1.5	0.032	248	260	−15.30	1.57	6.41
	60		50	1.4	0.066	226	244	−33.33	1.05	6.67
	20	300	350	2.25	0.023	213	226	−22.22	3.14	2.12
DoF, 5 cm	20		225	2	0.033	166	168	−6.67	3.14	4.44
	20	500	150	1.74	0.024	195	220	2.04	3.14	6.67
	30		95	1.65	0.034	192	204	2.09	2.09	7.01
Submerged adsorption column, 5 cm										
UpF	20	300	380	1.98	0.02	267	288	5.13	3.14	2.63
DoF			250	1.6	0.023	226	237	−28.5	3.14	4.00
UpF		500	250	2.1	0.02	335	341	−11.15	3.14	3.85
DoF			180	1.9	0.034	231	235	3.75	3.14	5.55
UpF	30		175	1.83	0.026	322	322	−16.1	2.09	4.30
	40		145	1.71	0.034	309	315	−26.3	1.57	4.55
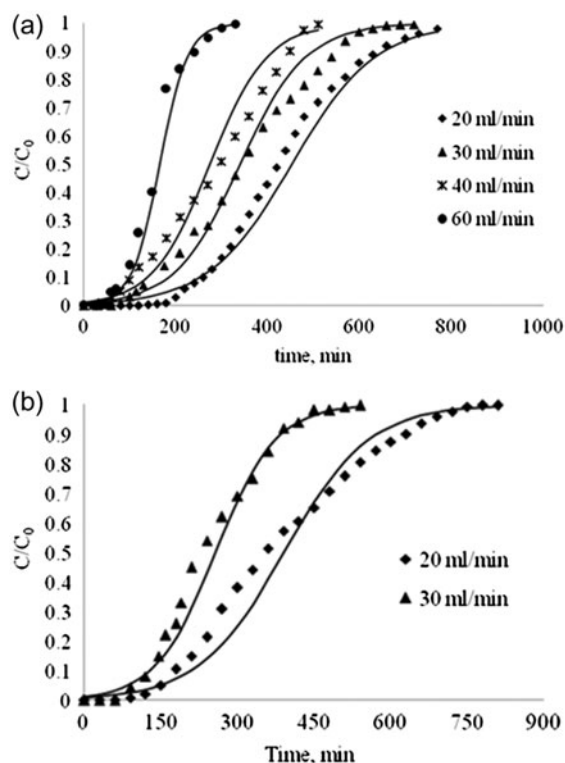
Fig. 3. Effect of flow rates of FBA: breakthrough curves of MB removal by JLP adsorbent predicted by Thomas model at $C_0 = 500$ mg/L and $H_T = 5$ cm for (a) up-flow mode with $Q = 20$, 30, 40, and 60 mL/min) and (b) down-flow mode with $Q = 20$ and 30 mL/min (symbols and lines correspond to experimental and theoretical values based on Eq. (9)).

UpF mode. On the contrary, the t_b was found to be 150 and 95 min for corresponding flow rates of 20 and 30 mL/min for DoF. For a smaller value of flow rate, the front of the adsorption zone reaches later to the top of the column for UpF and to the bottom of the column for DoF, thereby giving a higher t_b [17,34]. Thus, the usable bed height increases with decreasing flow rates. The adsorbent usage rate, U_r in the column is increased with the flow rates, which means a trace amount of adsorbent is required to treat unit volume of wastewater at lower flow rates. At 500 mg/L, concentration of the dye, and 5 cm column height, the U_r values increased from 4.89 to 6.67 g/L with the increase in flow rates from 20 to 60 mL/min for UpF, besides the increment obtained from 6.67 to 7.01 g/L for the flow rates of 20 to 30 mL/min for DoF. An increase in flow rates appears to increase the sharpness of the breakthrough curve. These results indicate that, as Q increases, the shape of the breakthrough curve changes dramatically from an S-shape to a downwardly concave shape. The curves exhibit a sharp leading edge and a broad tailing edge. The breadth of the tailing edge is most likely due to slow intraparticle diffusion within the pores of the JLP [35]. Both UpF and DoF columns show similar trends regarding the effects of Q on column parameters. In general, the adsorption capacity (q_{eq}) of JLP for MB decreases with the increase in flow rates and this effect is predominant for UpF. The values of q_{eq} increase up to 40% for UpF compared to that for DoF mode may be due to the slight expansion in JLP particles and voidage among the adsorbent particles as well as increase in bed heights so that MB cations might get enough space to adsorb on the JLP surface.

The velocity of the influent remarkably affected the contact between MB and JLP. At lower flow rates, the dyes have longer contact time with the adsorbent which results in a higher overall removal rate of dyes from the wastewater and the breakthrough curves were broaden due to the larger mass transfer zone. At higher flow rates, the breakthrough time for the column was shorter and the mass transfer zone was smaller. Similar results have also been reported by other researchers [36–38]. As the contact period between both the adsorbate and adsorbent was relatively short with the increased flow, the adsorption was not complete and led to steep breakthrough results at the beginning of the operation [32,39]. Our group also reported earlier that flow rates are inversely related to t_b as well as q_{eq} [5].

3.1.3. Effect of initial concentrations

The breakthrough curves of the FBA column with UpF and DoF modes were obtained by varying initial
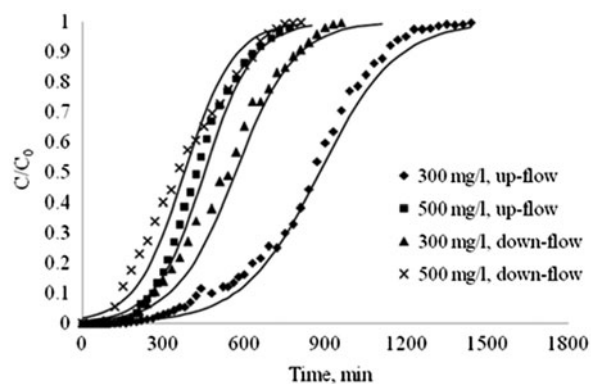

Fig. 4. Effect of initial concentrations of FBA: breakthrough curves of MB removal by JLP adsorbent predicted by Thomas model for up-flow and down-flow modes with $C_0 = 300$ and 500 mg/L at $Q = 20$ mL/min and $H_T = 5$ cm (symbols and lines correspond to experimental and theoretical values based on Eq. (9)).

MB concentrations in the range of 300–500 mg/L at constant flow rates (Fig. 4 and Table 2). It can be seen that the values of t_b decreased from 350 to 205 min, whereas, that of q_{eq} showed increment from 213 to 273 mg/g with the change in C_0 from 300 to 500 mg/L for $H_T = 5$ cm, $Q = 20$ mL/min, and UpF mode. Hence, the treated volume of wastewater is increased with the decrease in C_0 which explains the right shift of the breakthrough curves in Fig. 4 [40,41].

At lower initial concentrations, the slopes of the breakthrough curves were lower than that obtained at higher concentrations, indicating a relatively wider mass transfer zone and longer processing time. Moreover, it can be seen from the Table 2 that the adsorbent usage rate decreased from 4.89 to 2.12 g/L with the decrease in C_0 from 500 to 300 mg/L. These results demonstrate that the change in concentration gradient affects the saturation rate and processing time [36,37,42] followed by Fickian diffusion for mass transfer during adsorption between MB–JLP systems. This gradient results in the diffusion flux, J (mol/m^2.s) of the species, i.e. the rate of diffusion of MB through unit cross-section of the media (JLP) at the direction of the concentration gradient (dC/dx). JLP always creates a deviation in concentration gradient (dC/dx) defined as the driving force for MB adsorption in the system until it attains breakthrough. Guo et al. [3] carried out critical flux experiments for membrane separation system and reported that values higher than critical flux (20 L/m^2 h) reduce membrane fouling. In our case, there is no chance of fouling, nevertheless, the activity of the adsorbent decreases with operation time. Therefore, JLP adsorbent requires regeneration after a certain period of the ongoing operation. The effect of dC/dx is initially higher owing to the contact of fresh MB solution with JLP adsorbent and mass transfer is privileged due to fast front propagation of the MB cations toward its movement at higher velocity. Then, the driving force of the system gradually decreases until it reaches saturation. Adsorption rate increases with larger differences in concentration, shorter sorption path, greater medium permeability, and lower temperatures [33].

3.2. Effect of flow patterns

The effect of flow patterns on column performances have been investigated for the first time and the results are summarized in Table 2. It can be seen from the table that the UpF shows better performance than DoF under the same experimental conditions. The experimental data of FBA display that t_b decreased from 350 to 225 min (35.71%) as the flow pattern changed from UpF to DoF mode at
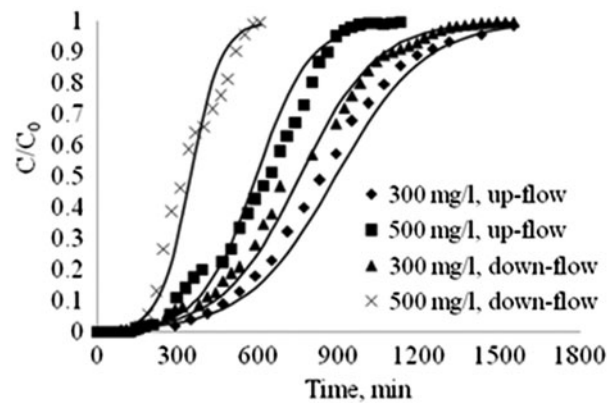

Fig. 5. Effect of initial concentrations of SA: breakthrough curves of MB removal by JLP adsorbent predicted by Thomas model for up-flow and down-flow modes with $C_0 = 300$ and 500 mg/L at $Q = 20$ mL/min and $H_T = 5$ cm (symbols and lines correspond to experimental and theoretical values based on Eq. (9)).

$Q = 20$ mL/min and $C_0 = 300$ mg/L. The equilibrium capacity for the UpF is also considerably higher (40%) than that of the DoF. At the same flow rate and $C_0 = 500$ mg/L, q_{eq} increased from 195 to 273 mg/g as t_b delayed 36.67% and H_B increased 20.70%; however, U_r decreased 36.40% and EBCT (3.14 min) and Thomas constant (k_{TH}, 0.02 mL/mg min) did not show any remarkable change when altering the mode from DoF to UpF. The reasons behind the better results for UpF excepting higher q_{eq}, t_b, and H_B depend on careful observation of the flow patterns (Fig. 5). The UpF patterns at $C_0 = 300$ and 500 mg/L are almost S-shaped and the slopes of the patterns are close to each other. However, the DoF patterns at the same conditions are quite different to one another, which may point out the effect of flow arrangements.

Additionally, the equilibrium forces for liquid–solid interactions in fluidized beds and mass transfer properties of the system have been studied in order to understand the effect of flow arrangements. For a bed of solid particles to be in the fluidized state, the total interaction forces exerted on it must match its weight. In the case of a single particle in an infinite expansion state ($\varphi = 1$), the total interaction can be conveniently divided into the drag force (F_d) and the buoyant force (F_b):

$$V_p \rho_p g = F_d + F_b \tag{11}$$

where V_p—particle volume (m^3), ρ_p—apparent particle density (kg/m^3), and g—gravitational acceleration constant (m/s^2). Yang and Renken [22] studied the

expansion of fluidized bed with the fluid velocity, the well–known Richardson–Zaki equation, applied to develop a more accurate relationship linking the apparent drag force F_d, buoyant force, F_b, the effective gravitational force, F_g between the particle and the liquid, and the voidage (φ) of fluidized beds under intermediate regime. The ratio of effective gravitational force (F_g) of fluid acting on an isolated single particle to the drag force (F_d), i.e. F_g/F_d is a function of voidage (φ) in multi-particle liquid fluidized bed. The equation $F_d = F_g f(\varphi)$ has been solved by Richardson–Zaki equation and reported the range of bed voidage $0.4 < \varphi < 1$ for best correlation between them in a liquid–solid fluidization process.

Based on the study, the role of UpF and DoF pro liquid–solid adsorption may be explained by the effect of the three forces, e.g. F_g, F_b, and F_d. If the sum of the both buoyancy and drag forces is greater than the force of gravity ($F_b + F_d > F_g$), the object will move up. As the column bed is fixed, adsorbent particles are more compact. Nevertheless, due to fluidized bed, these forces may assist both external and internal diffusion in a heterogeneous system, elucidated by Fogler [21]. In the first step, diffusion takes place from the bulk fluid to the external surface of the adsorbent. The adsorbate molecules, in the second step, diffuse from the external surface into and through the pores within the adsorbent (Fig. 6(c)). It is known that the
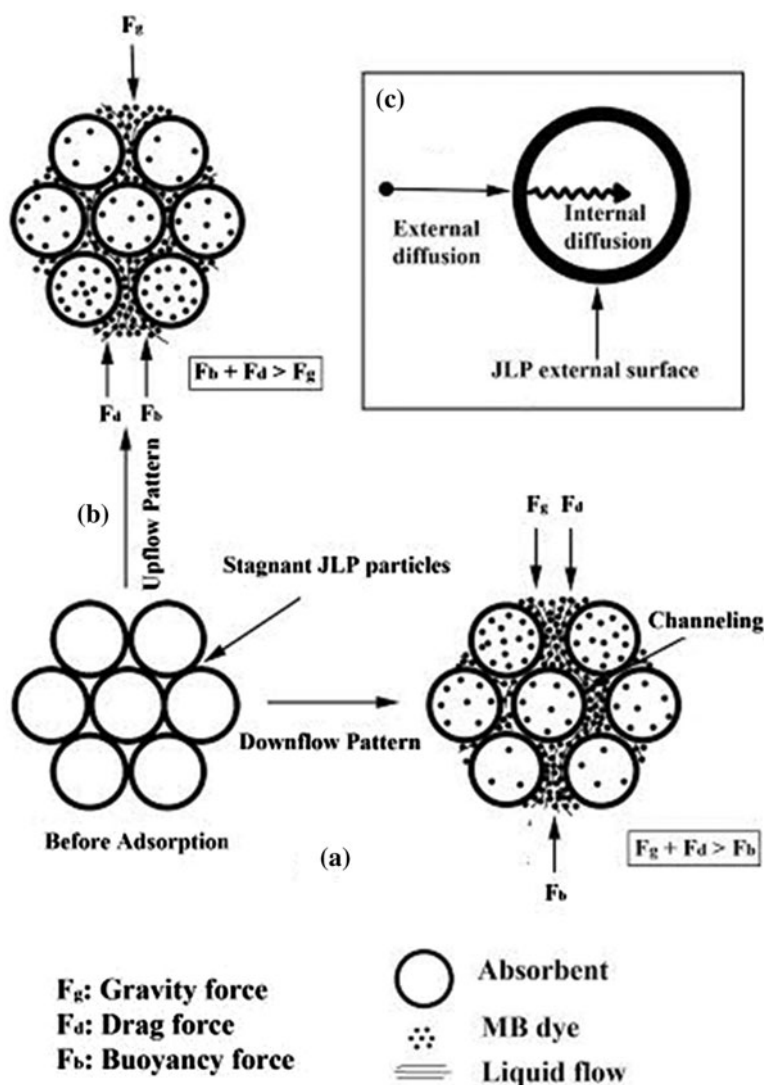

Fig. 6. Schematic diagram of the predictable adsorption mechanism of MB–JLP interaction in fluidized beds assisted by equilibrium forces (F_g, F_d, and F_b) for (a) down-flow with possible channeling ($F_g + F_d > F_b$) (b) up-flow with homogeneous diffusion ($F_b + F_d > F_g$), and (c) diffusion mechanism.

concentration of MB at the pore mouth must be higher than that inside the pore. Consequently, the entire JLP surface is not accessible to the same concentration; therefore, the rate of diffusion throughout the adsorbent will vary. The effective diffusivity (D_e) accounts for the fact that (a) not all of the area occupied by solids normal to the direction of the flux is available for the molecules to diffuse, (b) the paths of internal diffusion are tortuous, and (c) the pores are of varying cross-sectional areas. These parameters are interlinked to define D_e with an equation described in details in the reference [21], which can be applied to understand the diffusion mechanism of MB–JLP system. The rate of mass transfer to the surface is equal to the net rate of diffusion on and within the adsorbent.

In addition, UpF may create expansion of the bed and randomness of JLP particles resulting in better contact between the adsorption molecules (Fig. 6(b)) as well as better results for overall effective diffusivity by means of the dual effect ($F_b + F_d$) prevailing over the force of gravity. On the contrary, for DoF, the gravity force which shows major effect on the JLP adsorbent ($F_g + F_d > F_b$), may reduce contact area by contraction of bed and ready existence of channeling and the adsorbent molecules is not assembled properly in the column (Fig. 6(a)).

It may also be considered that a column of fluid-containing solid particles experiences greater pressure at the bottom of the column than at the top. This difference in pressures tends to accelerate an object upward. As pressure increases with depth in the column of aqueous solution of MB, the bottom particles undergo higher buoyancy force (F_b) to overcome the pressure and the force of gravity for UpF. Thus, the driving force may contribute to internal diffusion [20].

3.3. Performance of submerged adsorption module

On the way of technological advancement, a new approach named "submerged adsorption" has been developed for wastewater treatment. The schematic diagram of the system has been shown in the Fig. 1.

3.3.1. Effect of initial concentrations

The breakthrough curves of the SA module for both UpF and DoF arrangements at initial concentrations of 300 and 500 mg/L are presented in Fig. 5. The breakthrough time, t_b, for the $C_0 = 300$ and 500 mg/L, and $Q = 20$ mL/min was found to be 380 and 250 min, respectively for UpF and the corresponding values obtained 250 and 180 min for DoF. The saturation of the bed occurred faster at higher C_0, and hence adsorption capacity (q_{eq}) of the column increased. At
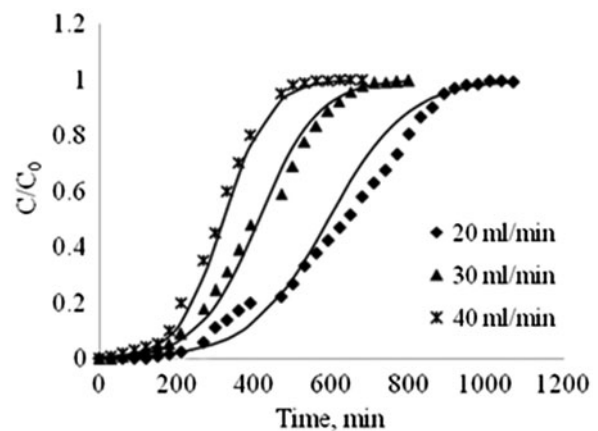

Fig. 7. Effect of flow rates of SA: breakthrough curves of MB removal by JLP adsorbent predicted by Thomas model for up-flow and down-flow arrangements with $Q = 20$, 30, and 40 mL/min at $C_0 = 500$ mg/L and $H_T = 5$ cm (symbols and lines correspond to experimental and theoretical values based on Eq. (9)).

higher concentration, more adsorbent is needed to adsorb higher amounts of dye in wastewater. Therefore, the adsorbent usage rate (U_r) increased with increasing the initial dye concentration.

3.3.2. Effect of volumetric flow rates

MB adsorption in SA column from a feed solution of 500 mg/L was tested at three flow rates 20, 30, and 40 mL/min (Fig. 7). The figure shows that the breakthrough curves shifted toward the origin with increasing flow rates. Lower flow rates result in higher residence times in the column and also higher breakthrough time (t_b) and higher usable bed heights (H_B). The t_b decreased from 250 to 145 min and H_B decreased from 2.1 to 1.71 cm with the increase in flow rates from 20 to 40 mL/min. The usage rate (U_r) increased with flow rates (Q), but adsorption capacity (q_{eq}) decreased through the SA column. For the conditions $Q = 20$ mL/min and $C_0 = 500$ mg/L, q_{eq} increased 45.02% as t_b held up 38.89%, and H_B increased 10.53%; however, U_r decreased 44.16% and EBCT and k_{TH} remained almost unchanged with altering the mode from DoF to UpF. The deviation () between the experimental and theoretical times for breakthrough and the experimental values of adsorption capacity (q) are also shown in the Table 2.

3.4. A new and effective approach

A new and effective approach concerning SA has been proposed instead of SMA process for wastewater

treatment. SMA technique is a pretreatment to bioreactor or reverse osmosis, which experiences a major problem of fouling leading to serious decline in the flux and quality of permeate, ultimately resulting in an adverse effect on sorption performance [43]. The process, in addition, undergoes complex technology, runs with discontinuous flow, readily clogged, needs regular maintenance, creates ecological problem as well as high energy consuming, is and expensive. A number of initiatives has been taken to overcome the shortcomings, e.g. microbial decomposition of organic pollutants [4], addition of powder activated carbon [44], etc., but they do not meet the present expectation. Therefore, we propose a simple, continuous, energy saving, low-cost and effective process named submerged adsorption for the first time instead of complicated membrane technology. The new approach does not need any mechanical device to flow water in the submergible tank in order to uphold a constant static head in the adsorption column. A pump has been shown in the Fig. 1; however, wastewater can be supplied in the submergible tank from a storage tank placed above the tank. The column made of simply PVC tube was filled with low-cost adsorbent (JLP). Design parameters of SA column in comparison to the conventional FBA found that q_{eq} increased up to 22.71% as well as H_B and t_b increased 9–14% and 20–86%, respectively. The equilibrium adsorption capacity is also higher (335 mg/g for $Q = 20$ mL/min and $C_0 = 500$ mg/L). There is no possibility of fouling and no external energy is required. Environmental pollution may cause during adsorbate–adsorbent interaction in tolerable range. Nevertheless, process control accessories are obliged for continuous level control in the column. Concluding remark is that SA module shows better performances for UpF, may be due to the generation of more effective surface area for cationic dye adsorption on the surface penetrated by net force as already explained.

4. Conclusion

The performance of submerged adsorption column over the conventional fixed bed one for wastewater treatment has been demonstrated quite effectively and proposed to be applied as an alternative to a rather complicated submerged membrane separation system. Different design parameters of the adsorption columns were extracted for UpF and DoFs based on bed depths (5–10 cm), flow rates (20–60 mL/min), and initial dye concentrations (300–500 mg/L). The UpF showed better performance than that of the DoF under the same experimental conditions. With

increase in the adsorption bed depths as well as initial dye concentrations and decrease in flow rates for any flow pattern, the breakthrough curves became broader and the adsorption capacity of the column increased as the breakthrough time and usable bed height increased. In addition, SA has been demonstrated in this context as a new, continuous, and cost-effective process because no mechanical device was required for liquid flow, only static head is enough to pass the water through the bed. Thomas model for the adsorption of MB onto JLP was used to predict the breakthrough curves under varying experimental conditions. This model showed good agreement between experimental and calculated breakthrough curves and proved the validity of the prediction. However, we have presented our preliminary results in this manuscript; further improvements in SA column design with regeneration method vis-à-vis sustainable chemical and biological treatment of industrial wastewater are under investigation.

References

[1] Y. Orem, R. Messalem, E. Ben-David, M. Herzberg, A. Kushmaro, X. Ji, G. Di Profio, E. Curcio, E. Drioli, J. Laroche, P.-J. Remize, J. Leparc, S. Vigneswaran, K. Chinu, M.A. Johir, J. Lee, H. Shon, J. Kandasamy, Y. Ye, L. Sim, B. Herulah, V. Chen, A. Fane, C. Tansakul, S. Laborie, C. Cabassud, Evaluation and comparison of seawater and brackish water pre-treatment, IWA, London, 2001.

[2] T. Lebeau, C. Lelièvre, H. Buisson, D. Cléret, L.W. Van de Venter, P. Côté, Immersed membrane filtration for the production of drinking water: Combination with PAC for NOM and SOCs removal, Desalination 117 (1998) 219–231.

[3] W. Guo, S. Vigneswaran, H.-H. Ngo, W. Xing, P. Goteti, Comparison of the performance of submerged membrane bioreactor (SMBR) and submerged membrane adsorption bioreactor (SMABR), Bioresour. Technol. 99 (2008) 1012–1017.

[4] S. Jeong, G. Naidu, S. Vigneswaran, Submerged membrane adsorption bioreactor as a pretreatment in seawater desalination for biofouling control, Bioresour. Technol. 141 (2013) 57–64.

[5] M. Tamez Uddin, M. Rukanuzzaman, M. Maksudur Rahman Khan, Adsorption of methylene blue from aqueous solution by jackfruit (Artocarpus heteropyllus) leaf powder: A fixed-bed column study, J. Environ. Manage. 90 (2009) 3443–3450.

[6] A.P. Lim, A.Z. Aris, Continuous fixed-bed column study and adsorption modeling: Removal of cadmium (II) and lead (II) ions in aqueous solution by dead calcareous skeletons, Biochem. Eng. J 87 (2014) 50–61.

[7] A.B. Albadarin, C. Mangwandi, A.H. Al-Muhtaseb, G.M. Walker, S.J. Allen, M.N.M. Ahmad, Modelling and fixed bed column adsorption of Cr(VI) onto orthophosphoric acid-activated lignin, Chin. J. Chem. Eng. 20 (2012) 469–477.

[8] A.A. Ahmad, B.H. Hameed, Fixed-bed adsorption of reactive azo dye onto granular activated carbon prepared from waste, J. Hazard. Mater. 175 (2010) 298–303.

[9] O. Hamdaoui, Batch study of liquid-phase adsorption of methylene blue using cedar sawdust and crushed brick, J. Hazard. Mater. 135 (2006) 264–273.

[10] V. Vadivelan, K.V. Kumar, Equilibrium, kinetics, mechanism, and process design for the sorption of methylene blue onto rice husk, J. Colloid Interface Sci. 286 (2005) 90–100.

[11] E. Demirbas, M. Kobya, S. Öncel, S. Şencan, Removal of Ni(II) from aqueous solution by adsorption onto hazelnut shell activated carbon: Equilibrium studies, Bioresour. Technol. 84 (2002) 291–293.

[12] R. Gong, Y. Sun, J. Chen, H. Liu, C. Yang, Effect of chemical modification on dye adsorption capacity of peanut hull, Dyes Pigm. 67 (2005) 175–181.

[13] K.V. Kumar, K. Porkodi, Relation between some two-and three-parameter isotherm models for the sorption of methylene blue onto lemon peel, J. Hazard. Mater. 138 (2006) 633–635.

[14] M. Doan, M. Alkan, A. Türkyilmaz, Y. Özdemir, Kinetics and mechanism of removal of methylene blue by adsorption onto perlite, J. Hazard. Mater. 109 (2004) 141–148.

[15] D. Ghosh, K.G. Bhattacharyya, Adsorption of methylene blue on kaolinite, Appl. Clay Sci. 20 (2002) 295–300.

[16] K.G. Bhattacharyya, A. Sharma, Kinetics and thermodynamics of methylene blue adsorption on neem (*Azadirachta indica*) leaf powder, Dyes Pigm. 65 (2005) 51–59.

[17] V.C. Srivastava, B. Prasad, I.M. Mishra, I.D. Mall, M.M. Swamy, Prediction of breakthrough curves for sorptive removal of phenol by bagasse fly ash packed bed, Ind. Eng. Chem. Res. 47 (2008) 1603–1613.

[18] A. Gürses, S. Karaca, Ç. Doğar, R. Bayrak, M. Açıkyıldız, M. Yalçın, Determination of adsorptive properties of clay/water system: Methylene blue sorption, J. Colloid Interface Sci. 269 (2004) 310–314.

[19] S.H. Lin, C.S. Wang, C.H. Chang, Removal of methyl tert-butyl ether from contaminated water by macroreticular resin, Ind. Eng. Chem. Res. 41 (2002) 4116–4121.

[20] Drag (physics). Available 23 August 2014 from: <http://en.wikipedia.org/wiki/Drag_force>.

[21] H.S. Fogler, Elements of chemical reaction engineering, fourth ed., Prentice Hall Professional Technical Reference USA, Massachusetts, 2005.

[22] J. Yang, A. Renken, A generalized correlation for equilibrium of forces in liquid–solid fluidized beds, Chem. Eng. J. 92 (2003) 7–14.

[23] J.R. Moate, M.D. LeVan, Fixed-bed adsorption with nonplug flow: Perturbation solution for constant pattern behavior, Chem. Eng. Sci. 64 (2009) 1178–1184.

[24] Z. Zhou, T. Zeng, Z. Cheng, W. Yuan, Kinetics of selective hydrogenation of pyrolysis gasoline over an egg-shell catalyst, Chem. Eng. Sci. 65 (2010) 1832–1839.

[25] S. Cay, A. Uyanik, A. Ozasik, Single and binary component adsorption of copper(II) and cadmium(II) from aqueous solutions using tea-industry waste, Sep. Purif. Technol. 38 (2004) 273–280.

[26] Z. Aksu, F. Gönen, Z. Demircan, Biosorption of chromium(VI) ions by Mowital®B30H resin immobilized activated sludge in a packed bed: Comparison with granular activated carbon, Process Biochem. 38 (2002) 175–186.

[27] C.Y. Yin, M.K. Aroua, W.M.A.W. Daud, Fixed-bed adsorption of metal ions from aqueous solution on polyethyleneimine-impregnated palm shell activated carbon, Chem. Eng. J. 148 (2009) 8–14.

[28] J.P. Chen, L. Wang, Characterization of metal adsorption kinetic properties in batch and fixed-bed reactors, Chemosphere 54 (2004) 397–404.

[29] K. Vijayaraghavan, J. Jegan, K. Palanivelu, M. Velan, Batch and column removal of copper from aqueous solution using a brown marine alga *Turbinaria ornata*, Chem. Eng. J. 106 (2005) 177–184.

[30] M.M. Nassar, Adsorption of Fe^{+3} and Mn^{+2} from ground water onto maize cobs using batch adsorber and fixed bed column, Sep. Sci. Technol. 41 (2006) 943–959.

[31] S. Bunluesin, M. Kruatrachue, P. Pokethitiyook, S. Upatham, G.R. Lanza, Batch and continuous packed column studies of cadmium biosorption by *Hydrilla verticillata* biomass, J. Biosci. Bioeng. 103 (2007) 509–513.

[32] X. Xu, B. Gao, X. Tan, X. Zhang, Q. Yue, Y. Wang, Q. Li, Nitrate adsorption by stratified wheat straw resin in lab-scale columns, Chem. Eng. J. 226 (2013) 1–6.

[33] C. Geankoplis, Transport processes and separation process principles (includes unit operations), Prentice Hall Press, New Jersey, NJ, 2003.

[34] G.Z. Kyzas, N.K. Lazaridis, M. Kostoglou, Modelling the effect of pre-swelling on adsorption dynamics of dyes by chitosan derivatives, Chem. Eng. Sci. 81 (2012) 220–230.

[35] D.O. Cooney, The importance of axial dispersion in liquid-phase fixed-bed adsorption operations, Chem. Eng. Commun. 110 (1991) 217–231.

[36] Z. Aksu, Ş.Ş. Çağatay, F. Gönen, Continuous fixed bed biosorption of reactive dyes by dried *Rhizopus arrhizus*: Determination of column capacity, J. Hazard. Mater. 143 (2007) 362–371.

[37] Y. Pamukoglu, F. Kargi, Biosorption of copper(II) ions onto powdered waste sludge in a completely mixed fed-batch reactor: Estimation of design parameters, Bioresour. Technol. 98 (2007) 1155–1162.

[38] A. Hatzikioseyian, M. Tsezos, F. Mavituna, Application of simplified rapid equilibrium models in simulating experimental breakthrough curves from fixed bed biosorption reactors, Hydrometallurgy 59 (2001) 395–406.

[39] K. Vijayaraghavan, J. Jegan, K. Palanivelu, M. Velan, Removal of nickel(II) ions from aqueous solution using crab shell particles in a packed bed up-flow column, J. Hazard. Mater. 113 (2004) 223–230.

[40] Z. Aksu, F. Gönen, Biosorption of phenol by immobilized activated sludge in a continuous packed bed: Prediction of breakthrough curves, Process Biochem. 39 (2004) 599–613.

[41] I. Iliuta, M.C. Iliuta, F. Larachi, Sorption-enhanced dimethyl ether synthesis—Multiscale reactor modeling, Chem. Eng. Sci. 66 (2011) 2241–2251.

[42] R. Han, Y. Wang, W. Zou, Y. Wang, J. Shi, Comparison of linear and nonlinear analysis in estimating the Thomas model parameters for methylene blue adsorption onto natural zeolite in fixed-bed column, J. Hazard. Mater. 145 (2007) 331–335.

[43] A. Matin, Z. Khan, S.M.J. Zaidi, M.C. Boyce, Biofouling in reverse osmosis membranes for seawater desalination: Phenomena and prevention, Desalination 281 (2011) 1–16.

[44] S. Jeong, T.V. Nguyen, S. Vigneswaran, Pretreatment of seawater for organic removal using powder activated carbon, IDA World Congress on Desalination and Water Reuse, Perth, (2011) 5–9.